



Title	PANI sensor for monitoring the oxidative degradation of wine using cyclic voltammetry
Author(s)	Begum, Parvin; Yang, Liu; Morozumi, Tatsuya; Sone, Teruo; Kawaguchi, Toshikazu
Citation	Food Chemistry, 414, 135740 https://doi.org/10.1016/j.foodchem.2023.135740
Issue Date	2023-07-15
Doc URL	http://hdl.handle.net/2115/92751
Rights	© 2023. This manuscript version is made available under the CC-BY-NC-ND 4.0 license http://creativecommons.org/licenses/by-nc-nd/4.0/
Rights(URL)	https://creativecommons.org/licenses/by-nc-nd/4.0/
Type	article (author version)
File Information	foodchem.2023.414.pdf



[Instructions for use](#)

1 **PANI sensor for monitoring the oxidative degradation of wine using cyclic**

2 **voltammetry**

3 Parvin Begum^{a*}, Liu Yang^b, Tatsuya Morozumi^a, Teruo Sone^{b,c}, Toshikazu Kawaguchi^a,

4 b

5 ^a Faculty of Environmental Earth Sciences, Hokkaido University, Sapporo 060-0810,

6 Japan

7 ^b Graduate School of Global Food Resources, Hokkaido University, Sapporo 060-8589,

8 Japan

9 ^c Faculty of Agriculture, Hokkaido University, Sapporo 060-8589, Japan

10 *Corresponding author

11 Email: parvinchy@ees.hokudai.ac.jp

12

13

14

15

16

17

1 **Abstract**

2 Redox species in wine are altered by pH and some wines are easily degraded due to
3 oxidation and sulfur dioxide (SO₂) reduction. There is a need for quick, easy, simple,
4 and economical methodologies for pH and wine-oxidized products (acetaldehyde)
5 analysis. This study aimed to measure pH and degradation of wines that were
6 electrochemically analyzed using polyaniline (PANI) sensor. Gas chromatography (GC)
7 and fourier transform infrared spectrometer (FT-IR) were also used. Electrochemical
8 analysis showed that oxidation was accelerated and peak currents ($I_{p,a}$) and potentials
9 ($E_{p,a}$) shifted to negative direction due to acetaldehyde formation. PANI sensor achieved
10 a limit of detection (LOD) of 7×10^{-1} ppm and a sensitivity of $5.20 \mu\text{A ppm}^{-1} \text{cm}^{-2}$.
11 Acetaldehyde formation was confirmed by GC (30%) and FT-IR spectra at 1647 cm^{-1} to
12 the C=O vibration of aldehyde. These results suggested that acetaldehyde degraded the
13 taste of wine after remaining open.

14

15 **Keywords**

16 Polyaniline sensor; Wine; Cyclic voltammetry; Degradation of wine

17

18 1. Introduction

19 Wine exposure to air/oxygen (O_2) can change wine from decent to inconsumable,
20 and its color can change from vibrant to brown-tinged, which is a sign of oxidation. The
21 pH of wine is another important factor, as it influences the stability of the wine's
22 microorganisms, protein solubility, affects color and oxidative reactions, and determines
23 the effectiveness of sulfur dioxide (SO_2) (Sarmiento et al., 2000). The alteration of color,
24 flavour, and taste are significantly influenced by polyphenols. Polyphenols can be
25 grouped into two families: (i) flavonoids (anthocyanidins, tannins, flavonols, flavanols,
26 flavanones, flavones) and (ii) non-flavonoids (hydroxycinnamic acids, hydroxybenzoic
27 acids, stilbenes etc). Polyphenols and organic acids readily oxidize into their
28 corresponding quinone in the presence of hydrogen per oxide (H_2O_2). Quinones affect
29 the color of wine, enhance its bitterness, and impair its flavor and nutritional value
30 (Marrufo-Curtido et al., 2022). Quinones can first undergo decarboxylation and then
31 hydrolysis to form an aldehyde. Quinones can also polymerize with flavonoids and
32 anthocyanins and form pigmented polymers, similar to acetaldehyde (Fowler et al.,
33 2011). Acetaldehyde is the major byproduct of wine oxidation and leads to changes in
34 color and flavor (Tarko et al., 2020). Researchers established that high temperatures and

35 excessive O₂ exposure cause wine to lose its rich flavors, color and taste (Ontañón, et al.,
36 2020). Acetaldehydes are well-known irritants that can cause headaches and dizziness if
37 inhaled over long periods, rapidly attach to proteins and DNA, and possibly even cause
38 cancer (Mizumoto et al., 2017). As a result, acetaldehyde is considered hazardous to the
39 environment, making its detection crucial. Unfortunately, consumers frequently ignore
40 these dangers. There are some time-consuming, expensive techniques used for the
41 detection of oxidized products (acetaldehyde.), such as high performance liquid
42 chromatography (HPLC), liquid chromatography-electrospray mass spectrometry
43 (LC-ES-MS), enzyme assay (Ontañón, et al., 2020, McCloskey and Mahaney, 1981),
44 spectroscopic techniques (ultraviolet (UV), infrared (IR)), etc.; those require trained
45 personnel. However, there aren't quick and easy ways to figure out how vulnerable
46 chemical composition of wine is to O₂ exposure or being left open for a long time.
47 Therefore, a quick, easy-to-use procedure that can reveal information about a wine's
48 susceptibility is required.

49 The formation of acetaldehyde (a carcinogen) in wine is well-known and favored
50 by exposure but can also develop in properly stored wines. This study aims to apply the

51 newly designed electrochemical PANI sensor to immediately understand the
52 deterioration of wine.

53 **2. Materials and methods**

54 *2.1. Wine samples and reagents*

55 Wines were procured from a local supermarket in Sapporo, Japan (Table 1).
56 Acetaldehyde causes a range of toxic, pharmacological, and behavioral responses (Guo
57 and Ren 2010) and is formed by the oxidation of ethanol in wine. After opening the
58 wine bottle, 50 mL of each wine was poured into a 100-mL beaker and remained open
59 at room temperature (± 25 °C) for 96 h to produce acetaldehyde, which was then
60 measured by a PANI sensor. Aniline was purchased from Sigma-Aldrich Co. LLC
61 (Tokyo, Japan), Sodium hydroxide (NaOH) and hydrochloric acid (HCl) (Wako Pure
62 Chem. Osaka, Japan)

63 Table 1. here

64 *2.2. Methods*

65 *2.2.1. Polyaniline sensor preparation*

66 The sensing electrode was a polyaniline-modified Au electrode prepared
67 previously described electro-polymerization method (Begum et al., 2021). A planar-type
68 electrochemical sensor chip (3.5 cm × 1.2 cm) developed by Hitachi Chem was cleaned
69 by ashing treatment using UV (172 nm, 10 mWcm⁻²) for 1 min. Aniline and perchloric
70 acid (HClO₄) (Wako Pure Chem. Osaka, Japan) were used to modify the chip. The chip
71 was modified via the electro-polymerization of PANI on the surface of the Au electrode
72 by applying a potential step of -0.025 V for 150 s in 1 M of aniline and 2 M of an
73 HClO₄ solution (Scheme SI-1). PANI can prevent the non-specific adsorption of
74 organic compounds onto the electrode.

75 2.2. 2. *Measurement of physiochemical parameter, CV, GC and FT-IR*

76 We measured the physiochemical parameter of the wine samples using OenoFoss
77 (Fourier Transform Infrared (FTIR)) (Web address). Table 1 showed the information of
78 wines accompanied with appearance/color and physiochemical parameters (pH, total
79 acid, volatile acid and total sugar) of red, rose, and white wines after 24 hours of the
80 opening using OneoFoss. The experimental configuration for CV measurement included
81 a planar-type electrochemical sensor chip with three electrodes—PANI/Au working, Au
82 counter, and Au pseudo-reference—all connected to a potentiostat, an IVIUM

83 COMPACTSTAT electrochemical interface, through a USB interface. Next, 50 μL of
84 wine (without any treatment) was dropped onto the sensing area at the working
85 electrode for CV measurement. All measurements were conducted at room temperature
86 (± 25 °C), with a scanning range of -0.1–0.7 V at the scan rate of 0.05 Vs^{-1} . The same
87 chip was used more than 100 times after being thoroughly washed with MilliQ water
88 (Begum et al., 2021). To create various pH wine solutions, NaOH and HCl were utilized.
89 The degradation of wines was electrochemically investigated using a PANI sensor and
90 analyzed them using CV. To test the PANI electrode's signal strength in the presence of
91 acetaldehyde, acetaldehyde (30, 35 and 40 ppm) and white wine were mixed and the CV
92 was recorded. The formation of acetaldehyde was confirmed by GC (SHIMADZU
93 GC-2025) according to the method (see supplementary information) reported by
94 Hübschmann. The formation of acetaldehyde was also determined by FT-IR (Nicolet iS
95 10, Thermo Scientific) following the procedure described by Kauffman et al.

96 *2.3. Statistical analysis*

97 Each experiment was conducted in triplicate. Statistical analysis was performed
98 using Student's t-test, with $P \leq 0.01$ (1 tail) considered significant. The experimental
99 results are presented as mean \pm SD (standard deviation).

100 3. Results and discussion

101 3.1. Effect of pH on the PANI sensor

102 The electrochemical parameters extracted from CV curve were the anodic and
103 cathodic peak currents ($I_{p,a}$ and $I_{p,c}$, respectively); anodic and cathodic peak potentials
104 ($E_{p,a}$ and $E_{p,c}$, respectively); peak-to-peak separation (ΔE_p); peak ratio and half-wave
105 potential. As shown in Fig. 1, both the oxidation and reduction peak potentials gradually
106 shift negatively with increasing pH, accompanied by a decrease in the peak area, which
107 is a consequence of the lower proton transfer involved in the oxidation process with
108 increasing pH. At high pH, the electrochemical potential of the wine solution was low,
109 and accordingly, an oxidation/reduction process occurred at a lower potential
110 concerning the PANI electrode. However, increasing the release of protons led to
111 acidification, increasing the electrical potential. These results are consistent with those
112 Fig. 1. here

113 of previous studies (Yakovleva et al. 2007). Yakovleva et al. (2007) observed that the
114 anodic peak voltage decreased with increasing pH, which was a consequence of the
115 decrease in the degree of antioxidant protonation and resulted in negative values. The
116 $E_{p,a}$ values for red wine (Fig. 1a) at pH 2 was 0.43 V, while the $E_{p,a}$ values of rosé (Fig.

117 1b) and white (Fig. 1c) wines were 0.25 and 0.36 V, respectively. Red wine contains
118 anthocyanins (red pigments), which have high reactivity under acidic conditions due to
119 the acidic character of the phenolic groups. A Reversible process was observed in all
120 cases. The electrochemical parameter E^0 shifted to more positive potentials as pH
121 decreased (Table SI-1). Anodic peak current decreased with increasing pH of red and
122 white wine as shown in Table (SI-1). At pH 2, 3, and 4, the oxidation and reduction
123 peaks were evident, however at pH 5 and even more so at pH 6, the electrochemical
124 reactions of the system were subdued. Thus, it is possible to explain the observed
125 pH-dependent redox reactions, in agreement with previous studies (Bourourou et al.,
126 2014).

127 The relationship between $E_{p,a}$ and the pH values in red wine was examined. The
128 linear regression equation was obtained as $E_{p,a}$ (mV) = 0.5294 - 0.055 pH, (n=3,
129 $R^2=0.9772$) (Fig. 1d). Value of the slope was close to the predicted value of 59 mV/pH,
130 demonstrating that the number of electrons and protons is equal (Murthy et al., 2019).
131 The relationship between E^0 and the pH values in rose and white wines were studied.
132 The plots produced showed a linear regression relationship with an equation E^0 (mV) =
133 0.2658 - 0.0289 pH, (n=3, $R^2=0.9897$) and E^0 (mV) =0.4242 - 0.0571 pH, (n=3,

134 $R^2=0.9997$) for rose and white wines respectively (Fig. 1e and 1f). The values (0.0289
135 (rose) and 0.0571 (white)) produced from the slope of E^0/pH of the regression line are
136 near to theoretical value/Nernstian value of 29.5 mV/pH and 59 mV/pH respectively
137 (Hong et al., 2006, Zhang et al., 2014), indicating that the number of electron and
138 protons involved in oxidation/reduction reaction for two-electron/one-proton and a
139 similar number of electron-proton process respectively. We used PANI sensor to
140 measure pH with Au electrode as a reference to avoid contamination of the main
141 electrolyte by the reference electrolyte, used at room temperature and no need to
142 equilibrate PANI sensor before use each time.

143 *3.2. CV measurement of red, rosé, and white wines immediately after opening*

144 First, the CV of six red, two rosé, and four white wines were measured
145 immediately after opening the bottle; the results are shown in Fig. 2. One anodic peak
146 Fig. 2. here

147 ($E_{p,a}$) was observed at around 0.35 V to 0.42 V and one cathodic peak ($E_{p,c}$) appeared at
148 around 0.11 V to 0.17 V on the first CV scan. The peak current and potential depend on
149 the concentration of redox-active molecules present in wine (Pwavodi et al., 2021). A
150 slight difference was observed in anodic/cathodic peak current and cathodic peak

151 potential from CV (Table SI-2). Alcohol and phenolic/organic components are the main
152 compounds in wines that may be expected to show redox activity towards PANI
153 electrode. Redox-active species in wine (such as flavanols, flavanol derivatives,
154 phenolic acids, SO₂, and ascorbic acid) interfere with the responses of CV. Phenolic
155 compounds in wines oxidized at a potential of less than 500 mV (Beer et al., 2004).
156 Organic acids in wine such as ascorbic acid, malic acid, tartaric acid, and caffeic acid
157 showed a large positive voltage range of 0.55 to 0.70 V with a height of the current peak
158 at 9.2 to 10.2 μA (Zhang et al., 2017). Makhotkina et al. (2010) demonstrated that the
159 $E_{p,a}$ greater than 0.35 V is owing to the presence of free SO₂ and with a further
160 contribution from catechol-containing phenolics such as caffeic acid derivatives and
161 catechin also possible. Catechol, one of the polyphenols found in wines did not show
162 redox activity toward PANI electrode (Begum et al., 2021). In a previous paper, we
163 showed that the anodic peak at around 0.35 V to 0.42 V and the cathodic peak at around
164 0.11 V to 0.17 V for the preservative, SO₂ (Begum et al., 2021). H₂S and organic
165 components were non-specifically deposited on the surface of the electrode; it is
166 challenging to obtain a stable electric signal for the measurement of wine. Wine
167 non-specific adsorption can be avoided using PANI (Begum, et al., 2019). The different
168 pH of the wine solutions also affected the oxidation/reduction on the surface of PANI

169 electrode. There was also no significant difference observed according to the FTIR
170 (OenoFoss) data (total acid, Table 1). $I_{p,a}$ value decreased with increasing pH of wine as
171 shown in Table 1 and Table (SI-2).

172 *3.3. CV measurement of red, rosé, and white wines after being open for several hours*

173 Fig. 3 shows the CVs of (a) red, (b) rosé, and (c) white wines after opening for
174 several hours. After opening at room temperature (± 25 °C), each wine lost its alcohol
175 concentration. Several wines open for 48–72 h showed little change, but most wines lost
176 their alcohol concentration quickly after opening, which caused the taste to subtly
177 change and become less vibrant after the first day; this was especially the case for white
178 wines, which tend to oxidize more quickly. Under the presence of O₂ for several hours
179 (24–72 h) at room temperature, white wines degrade easily. This leads to decreased
180 wine quality (e.g., a noticeable increase in sugar content) that affects public health. It is
181 well known that white wines are adversely affected by oxygen exposure, although many
182 red wines benefit from a certain degree of oxidation (Danilewicz, 2003). CV (Fig. 3d)
183 analysis suggested that the red wines did not change as much as white wines, which
184 may be because of the high amounts of tannin, polyphenol, and antioxidant present in
185 red wine that protects them from degradation even after 72 h. White wines are produced

186 by fermenting solely the grape juice, whereas red wines are produced using the skins
187 and seeds of the grapes. However, minor oxidation of the phenolic compounds in red
188 wine can help stabilize the color (Lopes et al., 2009). Acetaldehyde is produced as a
189 result of oxidation. This aldehyde formation provides the chemical bridge to bind
190 anthocyanins and tannins together in red wine. Tannins stabilize anthocyanins by
191 binding to form larger polymeric pigments.

192 Fig. 3. here

193 Antioxidants, anthocyanins in red wine can stabilize the beverage through
194 co-pigmentation, acetylation, and self-association (Kharadze et al., 2018). Acylated
195 anthocyanins, according to the researcher, can make red wine more stable (Alcalde-Eon
196 et al., 2006). Red wine's anthocyanin content is influenced by the grape's initial
197 anthocyanin profile and the winemaking methods used (Gonzalez-San Jose et al., 1990).
198 When being transported, stored, or left open, oxygen exposure and high temperatures
199 can have an impact on the quality of wines, particularly white wine (Ricci et al., 2017).
200 The anodic peak current of the red, rosé and white wines decreased with increasing time
201 of opening. Such decreases may be related to the formation of acetaldehyde.
202 Acetaldehyde is produced in wines when ethanol is oxidized in the presence of oxygen

203 from the atmosphere (Danilewicz, 2003). In nonenzymatic oxidation (enzyme removed
204 or inactivated), under the catalytic effects of iron (Fe^{2+}) and copper (Cu^+) ions,
205 molecular oxygen is reduced to its major radical, H_2O_2 . Iron is a natural component in
206 wines that are involved in metabolism as an enzyme activator and solubilizer. When
207 H_2O_2 is present, polyphenols and organic acids spontaneously oxidize into their
208 corresponding quinone (Voelker et al., 1996). Quinones can be converted to aldehydes
209 via hydrolysis after being first decarboxylated (Fowler et al., 2011). Naturally occurring
210 substances (eg, isobutanol) in wine are quickly oxidized to the corresponding aldehydes
211 and then transformed into acetic acid/vinegar. Acetaldehyde is a key potential toxin for
212 the development of alcoholic illnesses and causes a range of toxic, pharmacological and
213 behavioral responses (Guo and Ren 2010). As shown in Fig. 3d, white wines showed
214 significant changes. Thus, we checked several types of white wines after being left at
215 room temperature for a few days.

216 *3.4. CV of white wines after several hours of being open*

217 As shown in Fig. 4, the $I_{p,a}$ and $E_{p,a}$ values of (a) Chardonnay, (b) Niagara, (c)
218 Reisling, and (d) Sauvignon Blanc shift in a negative direction with time (0–96 h)

219 because of the decreasing number of electroactive functional groups and the increasing
220 number of oxidized products, such as acetaldehyde, in the wine solution; this result is in
221 agreement with those of previous literature (Makhotkina et al., 2010, Feng et al., 2014).
222 Depending on the wine composition, the peak potential and current values vary for
223 various wines. The new peak in the CV may be caused by the product of the oxidation
224 or reduction of the original wine components during the opening.

225 Fig. 4. here

226 In addition to the redox molecules of wine, the CV peak also depends on the pH
227 level of the wine (Makhotkina et al., 2010, Feng et al., 2014). With time after opening,
228 the pH of rose wine dropped (pH 3.28 after immediately opening and 3.00 after 72h). At
229 lower pH, pairs of peaks appeared to migrate closer and merge into a single broad peak
230 at higher pH (Feng et al., 2014). The combination of numerous phenolic antioxidants in
231 wine with various formal potentials may also have contributed to the broadness of the
232 peaks (Piljac et al., 2004). The larger-sized phenolic compounds that result from the
233 original wine phenolics' oxidation during storage—which is what causes the brown
234 colors to appear—could also undergo a different type of oxidation and contribute to the

235 second peak in the CV of wines. After being left open for several hours, white niagara
236 and white sauvignon blanc displayed (Figs. 4b and 4d, respectively) a decrease in the
237 anodic current and a modest increase in the cathodic current. According to Makhotkina
238 et al. (2010), the quick interaction of all the free SO₂ with acetaldehyde causes the
239 anodic current to diminish and the cathodic current to slightly increase. CV is a quick
240 way to assess the susceptibility of wine that will give the wine drinker useful
241 information and can become an alternative to traditional spectrophotometric techniques
242 (Makhotkina et al., 2010).

243 3.5. *Detection of acetaldehyde*

244 Acetaldehyde and the wine preservative SO₂ have a strong binding relationship,
245 as previously described (Schneider et al., 2014). After many hours of opening the wine,
246 a noticeably decreased sensing current was seen, which may be related to SO₂ binding
247 to acetaldehyde. Previously reported that aldehyde was formed by wine oxidation. The
248 formation of aldehyde depends on the oxidation time, pH, and chemical composition of
249 wine (Bueno et al., 2018 and Marrufo-Curtido et al., 2022). As demonstrated in Fig.
250 SI-1, when white wine and acetaldehyde were mixed, the $I_{p,a}$ value increased with
251 decreasing acetaldehyde content. The behavior is influenced by the composition of wine

252 and the research environment. Fig. 5 shows the results of the calibration curve of the
253 PANI sensor at acetaldehyde concentrations of 30–40 ppm versus anodic peak
254 current: $I_{p,a} (\mu\text{Acm}^{-2}) = 2.1541 - 0.0411C$ ($R^2 = 0.9977$).

255 Fig. 5. here

256 Alcohol undergoes oxidation reactions that produce acetaldehydes, which can
257 then be further oxidized to produce acetic acid. The presence of the acetaldehyde band
258 in GC chromatogram confirmed the formation of acetaldehyde (after 12 h (30%), 24 h
259 (21%) and decreased to 5% after 48 h) in wine. The presence of the band at 1647 cm^{-1}
260 in FT-IR spectra was assigned to the C=O vibration of aldehyde which confirmed the
261 formation of acetaldehyde in wine (after 24 h). Acetic acid content becomes more
262 significant at higher pH levels (Agatonovic-Kustrin et al., 2013). pH and volatile acid
263 increased with time, according to FTIR (OneoFoss) measurements. The CV of grape
264 juice that contained acetic acid was used to investigate the influence on the
265 electrochemical in the PANI sensor. CV of grape juice and white wine (after 96 h)
266 showing similar oxidation or reduction peaks; the acetic acid (data not shown) may have
267 been produced in white wine (after 96 h).

268 *3.5.1. Repeatability, reproducibility, limit of detection (LOD), and sensitivity*

269 Repeatability was determined by replicate CV analysis using the PANI sensor of
270 one original white wine (immediately after opening, $n = 3$) and the relative standard
271 deviations (RSD) of the peak currents were found to be 0.7%, indicating adequate
272 repeatability. The reproducibility of the sensor was investigated by the CV analysis of
273 the same wine using three different chips ($n = 3$). The low RSD value (1.1%) of the
274 peak currents indicates that the PANI electrode is highly reproducible. The LOD of $7 \times$
275 $10^{-1} \text{ mol.L}^{-1}$ of the current sensor was determined from the calibration curve (Figure 5).
276 This was calculated using the value of the slope of the curve and standard deviation (SD,
277 $n=3$) ($\text{LOD} = 3 \cdot \text{SD} / \text{slope}$). The sensitivity toward acetaldehyde is evaluated by
278 measuring the slope of the calibration curve (Fig. 5) and dividing it by the area of PANI
279 electrode. The sensitivity of $5.20 \mu\text{A ppm}^{-1} \text{ cm}^{-2}$ is obtained for PANI sensor for the
280 detection of acetaldehyde. The obtained LOD with PANI electrode is comparable to
281 recent works (Table SI-3) (Ahammad et al., 2016, Zhang et al., 2014, Ocampo et al.,
282 2018, Hosseini et al., 2005, Zhang et al., 2016, Do and Wang, 2013).

283 **4. Conclusions**

284 In conclusion, data from CV confirm that wine undergoes vital changes after
285 being continuously open at room temperature (± 25 °C) for several hours (72–96 h). As
286 expected, the differences induced by the availability of oxygen and temperature are
287 strongly linked to the oxidation reaction, which triggers the accumulation of the
288 oxidized product (e.g., acetaldehyde, confirmed by GC and FTIR) that readily binds
289 with SO₂ and can be detected with our PANI sensor. This method provides a simple
290 one-step technique to create a very low-cost electrode compared to other sensors being
291 used to analyze wine, eliminates any post-processing steps, easy to use and more
292 sensitive and selective than spectrometric methods. These results would be informative
293 for wine drinkers. Further study is required for visualizing the changes in wine
294 components using PANI sensor.

295 **Acknowledgments.** The very helpful comments from the reviewers on the
296 preliminary version of this paper are gratefully acknowledged. Shenxing Wang is
297 thanked for his technical assistance. The authors thank to Professor Yuichi Kamiya and
298 Professor Shin-ichiro Noro for support on GC-MS and FT-IR analysis of wines
299 respectively.

300 **Funding.** This work was funded by ROBUST and Hitachi Chemical, which is
301 gratefully acknowledged.

302 **Supplementary Data**

303 All datasets generated for this study are included in the article/supplementary material.

304 **Author contributions.** Toshikazu kawaguchi and Parvin Begum conceived and
305 planned the experiments. Parvin Begum carried out the experiment, performed the
306 analysis, drafted the manuscript, and designed the figures. Liu Yang helped to
307 experiment. All authors discussed the results and commented on the manuscript.

308 **Ethical approval** This article does not contain any studies with human and/or animal
309 participants performed by any of the authors.

310 **References**

311 Agatonovic-Kustrin, S., Morton, D. W., & Yusof, A. P. Md. (2013). The use of
312 Fourier Transform Infrared (FTIR) spectroscopy and Artificial Neural Networks
313 (ANNs) to assess wine quality. *Modern Chemistry and Applications, 1*, 110. DOI:
314 10.4172/2329-6798.1000110.

315 Ahammad, A. J. S., Mamun, A. A., Akter, T., Mamun, M. A., Faraezi, S., & Monira,
316 F. Z. (2016). Enzyme-free impedimetric glucose sensor based on gold

317 nanoparticles/polyaniline composite film. *Journal of Solid State Electrochemistry*,
318 20, 1933–1939. DOI 10.1007/s10008-016-3199-2.

319 Alcalde-Eon, C., Escribano-Bailón, M. T., Santos-Buelga, C., & Rivas-Gonzalo, J.
320 C. (2006). Changes in the detailed pigment composition of red wine during maturity
321 and ageing: A comprehensive study. *Analytica Chimica Acta*, 563, 238–254.
322 <https://doi.org/10.1016/j.aca.2005.11.028>.

323 Begum, P., Li, S., Morozumi, T., Johmen, M., Sone, T., & Kawaguchi, T. (2019).
324 Electrochemical sensing for analysis of wine. *Proceedings of Chemical Sensor
325 Symposium*, 35, 49–51.

326 Begum, P., Morozumi, T., Kawaguchi, T., & Sone, T. (2021). Development of an
327 electrochemical sensing system for wine component analysis. *ACS Food
328 Science & Technology*, 1, 2030–2040.
329 <https://doi.org/10.1021/acsfoodscitech.1c00146>.

330 Beer, D. De., Harbertson, J. F., Kilmartin, P. A., Roginsky, V., Barsukova, T.,
331 Adams, D. O., & Waterhouse, A. L. (2004). Phenolics: A comparison of diverse
332 analytical methods. *American Journal of Enology and Viticulture*, 55, 389–400.
333 DOI: 10.5344/ajev.2004.55.4.389.

334 Bourourou, M., Barhoumi, H., Maaref, A., & Jaffrezic-Renault, N. (2014).
335 Electrochemical study of modified glassy carbon electrode with carboxyphenyl
336 diazonium salt in aqueous solutions. *Sensors & Transducers*, 27, 22–28.

337 Bueno, M., Marrufo-Curtido, A., Carrascon, V., Fernandez-Zurbano, P., Escudero,
338 A., & Ferreira, V. (2018). Formation and accumulation of acetaldehyde and strecker
339 aldehydes during red wine oxidation. *Frontiers Chemistry*, 6, 20.
340 <https://doi.org/10.3389/fchem.2018.00020>.

341 Danilewicz, J. C. (2003). Review of reaction mechanisms of oxygen and proposed
342 intermediate reduction products in wine: central role of iron and copper.
343 *American Journal of Enology and Viticulture*, 54, 73–85. Corpus ID: 87659513.
344 ISSN 0002-9254.

345 Do, J. S., & Wang, S. H. (2013). On the sensitivity of conductimetric acetone gas
346 sensor based on polypyrrole and polyaniline conducting polymers. *Sensors and*
347 *Actuators, B*, 185, 39–46. <https://doi.org/10.1016/j.snb.2013.04.080>.

348 Feng, X., Zhang, Y., Yan, Z., Ma, Y., Shen, Q., Liu, X., Fan, Q., Wang, L., &
349 Huang, W. (2014). Synthesis of polyaniline/Au composite nanotubes and their high

350 performance in the detection of NADH. *Journal of Solid State Electrochemistry*, 18,
351 1717–1723. 10.1007/s10008-014-2407-1.

352 Fowler, Z. L., Baron, C. M., Panepinto, J. C., & Koffas, M. A. G. (2011).
353 Melanization of flavonoids by fungal and bacterial laccases. *Yeast*, 28, 181–188.
354 <https://doi.org/10.1002/yea.1829>.

355 Gonzalez-San Jose, M. L., Santa-Maria, G., & Diez, C. (1990). Anthocyanins as
356 parameters for differentiating wines by grape variety, wine-growing region, and
357 wine-making methods. *Journal of Food Composition and Analysis*, 3, 54–66.
358 [https://doi.org/10.1016/0889-1575\(90\)90009-B](https://doi.org/10.1016/0889-1575(90)90009-B).

359 Guo, R., & Ren, J. (2010). Alcohol and acetaldehyde in public health: from marvel to
360 menace. *International Journal of Environmental Research and Public Health*, 7,
361 1285–1301. doi: 10.3390/ijerph7041285.

362 Hong, J., Ghourchian, H., & Moosavi-Movahedi, A. A. (2006). Direct electron
363 transfer of redox proteins on a nafion-cysteine modified gold electrode.
364 *Electrochemistry communications*, 8, 1572–1576.
365 <https://doi.org/10.1016/j.elecom.2006.07.011>.

366 Hosseini, S. H., Oskoei, S. H. A., & Entezani, A. A. (2005). Toxic gas and vapour

367 detection by polyaniline gas sensor. *Iranian Polymer Journal*, *14*, 333–344. Corpus
368 ID: 97048494.

369 Hübschmann, H. -J. (2015). *Handbook of GC-MS: fundamentals and applications*.
370 Wiley-VCH Verlag GmbH & Co. KgaA. Weinheim, Germany. ISBN:
371 9783527334742.

372 Kharadze, M., Japaridze, I., Kalendia, A., & Vanidze, M. (2018). Anthocyanins and
373 antioxidant activity of red wines made from endemic grape varieties. *Annals of*
374 *Agrarian Science*, *16*, 181–184. <https://doi.org/10.1016/j.aasci.2018.04.006>.

375 Kauffman, K. L., Culp, J. T., Goodman, A., & Matranga, C. (2011). FT-IR study of
376 CO₂ adsorption in a dynamic copper(II) benzoate–pyrazine host with CO₂–CO₂
377 interactions in the adsorbed state. *The Journal of Physical Chemistry C*, *115*,
378 1857–1866. <https://doi.org/10.1021/jp102273w>.

379 Lopes, P., Silva, M. A., Pons, A., Tominaga, T., Lavigne, V., Saucier, C., Darriet, P.,
380 Teissedre, P.-L., & Dubourdieu, D. (2009). Impact of oxygen dissolved at bottling
381 and transmitted through closures on the composition and sensory properties of a
382 sauvignon blanc wine during bottle storage. *Journal of Agricultural and Food*
383 *Chemistry*, *57*, 10261–10270. doi: 10.1021/jf9023257.

384 Makhotkina, O., & Kilmartin, P. A. (2010). The use of cyclic voltammetry for wine
385 analysis: determination of polyphenols and free sulfur dioxide. *Analytica*
386 *Chimica Acta*, 668, 155–165. <https://doi.org/10.1016/j.aca.2010.03.064>.

387 Marrufo-Curtido, A., Ferreira, V., & Escudero, A. (2022). Factors that affect the
388 accumulation of strecker aldehydes in standardized wines: the importance of pH in
389 oxidation. *Molecules*, 27, 3056; <https://doi.org/10.3390/molecules27103056>.

390 McCloskey, L. P., & Mahaney, P. (1981). An enzymatic assay for acetaldehyde in
391 grape juice and wine. *American Journal of Enology and Viticulture*, 32, 159–162.

392 Mizumoto, A., Ohashi, S., Hirohashi, K., Amanuma, Y., Matsuda, T., & Muto, M.
393 (2017). Molecular mechanisms of acetaldehyde-mediated carcinogenesis in squamous
394 epithelium. *International Journal of Molecular Science*. 18, 1943.
395 doi: 10.3390/ijms18091943.

396 Murthy, A. P., Duraimurugan, K., Sridhar, J., & Madhavan, J. (2019). Application
397 of derivative voltammetry in the quantitative determination of alloxan at
398 single-walled carbon nanotubes modified electrode. *Electrochimica Acta*, 317,
399 182–190. DOI: 10.1016/j.electacta.2019.05.163.

400 Ocampo, A. M., Santos, L. R., Julian, S., Bailon, M. X., & Bautista, J. (2018).
401 Polyaniline-based cadaverine sensor through digital image colorimetry. *e-Polymers*.
402 *18*, 465–471. <https://doi.org/10.1515/epoly-2018-0083>.
403 Ontañón, I., Sánchez, D., Sáez, V., Mattivi, F., Ferreira, V., & Arapitsas, P. (2020).
404 Liquid chromatography-mass spectrometry-based metabolomics for understanding
405 the compositional changes induced by oxidative or anoxic storage of red wines.
406 *Journal of Agricultural and Food Chemistry*, *68*, 13367–13379.
407 <https://doi.org/10.1021/acs.jafc.0c04118>.
408 Piljac, J., Martinez, S., Stipèeviæ, T., Petroviæ, Z., & Metikoš-Hukoviæ, M. (2004).
409 Cyclic voltammetry investigation of the phenolic content of Croatian wines.
410 *American Journal of Enology and Viticulture*, *55*, 4. ISSN : 0002-9254.
411 Pwavodi, P. C., Ozyurt, V. H., Asir, S., & Ozsoz, M. (2021). Electrochemical sensor
412 for determination of various phenolic compounds in wine samples using
413 Fe₃O₄ nanoparticles modified carbon paste electrode. *Micromachines* (Basel),
414 *12*, 312. doi: 10.3390/mi12030312.

415 Ricci, A., Parpinello, G. P., & Versari, A. (2017). Modelling the evolution of
416 oxidative browning during storage of white wines: Effects of packaging and
417 closures. *International Journal of Food Science & Technology*, *52*, 472–479.
418 <https://doi.org/10.1111/ijfs.13303>.

419 Sarmiento, M. R., Oliveira, J. C., Slatner, M., & Boulton, R. B. (2000). Influence of
420 intrinsic factors on conventional wine protein stability tests. *Food Control*, *11*,
421 423– 432.

422 Schneider, M., Türke, A., Fischer, W. -J., & Kilmartin, P. A. (2014). Determination
423 of the wine preservative sulfur dioxide with cyclic voltammetry using inkjet printed
424 electrodes. *Food Chemistry*, *159*, 428–432. doi: 10.1016/j.foodchem.2014.03.049.

425 Tarko, T., Duda-Chodak, A., Sroka, P., & Siuta, M. (2020). The impact of oxygen at
426 various stages of vinification on the chemical composition and the antioxidant and
427 sensory properties of white and red wines. *International Journal of Food Science*.
428 2020, Article ID 7902974, 1–11. doi: 10.1155/2020/7902974

429 Voelker, B. M., & Sulzberger, B. (1996). Effects of fulvic acid on Fe(II) oxidation
430 by hydrogen peroxide. *Environmental Science & Technology*, *30*, 1106–1114.
431 <https://doi.org/10.1021/es9502132>.

432 Yakovleva, K. E., Kurzeev, S. A., Stepanova, E. V., Fedorova, T. V., Kuznetsov, B.
433 A., & Koroleva, O. V. (2007). Characterization of plant phenolic compounds by
434 cyclic voltammetry. *Applied Biochemistry and Microbiology*, *43*, 661–668.
435 DOI:10.1134/S0003683807060166.

436 Zhang, J., Guan, P., Li, W., Shi, Z., & Zhai, H. (2016). Synthesis and
437 characterization of a polyaniline/silver nanocomposite for the determination of
438 formaldehyde. *Instrumentation Science & Technology*, *44*, 249–258.
439 <https://doi.org/10.1080/10739149.2015.1104507>.

440 Zhang, Q., Türke, A., & Kilmartin, P. (2017). Electrochemistry of white wine
441 polyphenols using PEDOT modified electrodes. *Beverages*, *3*, 28.
442 <https://doi.org/10.3390/beverages3030028>.

443 Zhang, S., Zhang, D., Sheng, Q., & Zheng, J. (2014). PANI–TiC nanocomposite
444 film for the direct electron transfer of hemoglobin and its application for biosensing.
445 *Journal of Solid State Electrochemistry*, *18*, 2193–2200. DOI
446 10.1007/s10008-014-2462-7.

447 Web address: Wine analysis instrument measures more than 10 process parameters

448 (fossanalytics.com)

449

450

451

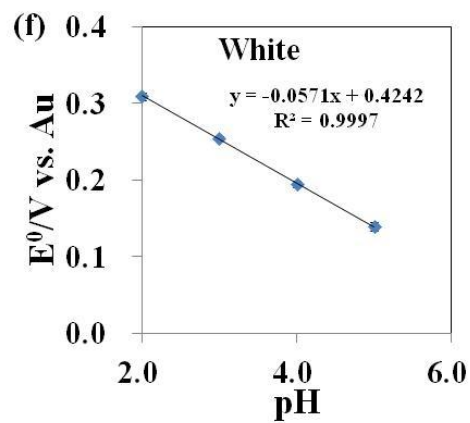
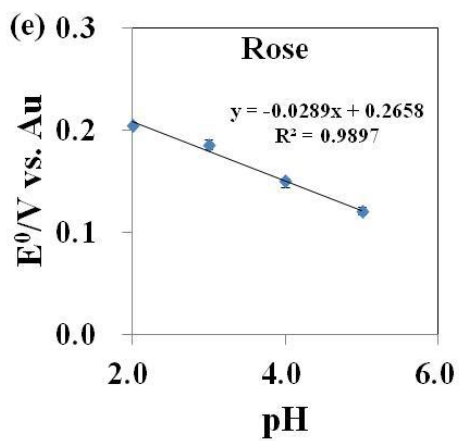
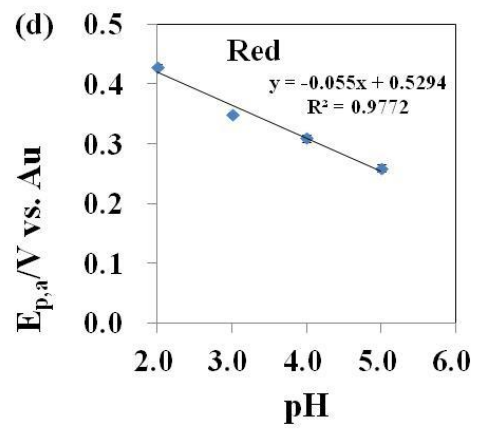
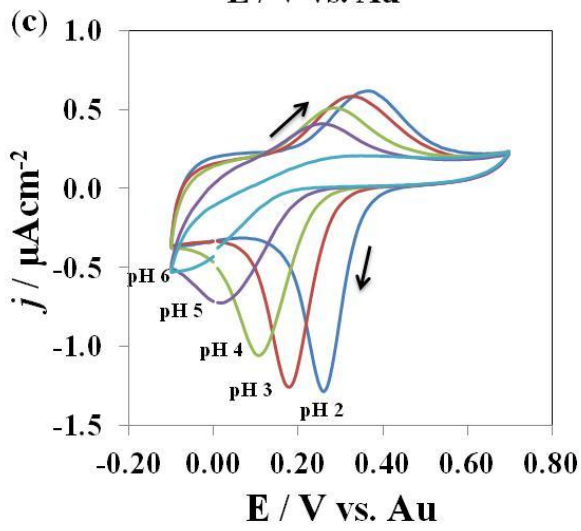
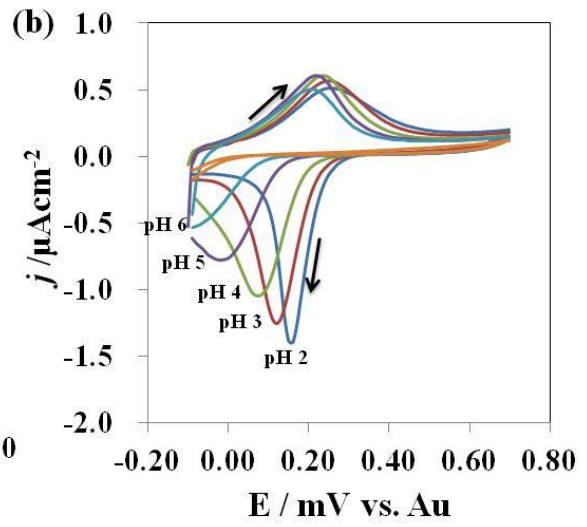
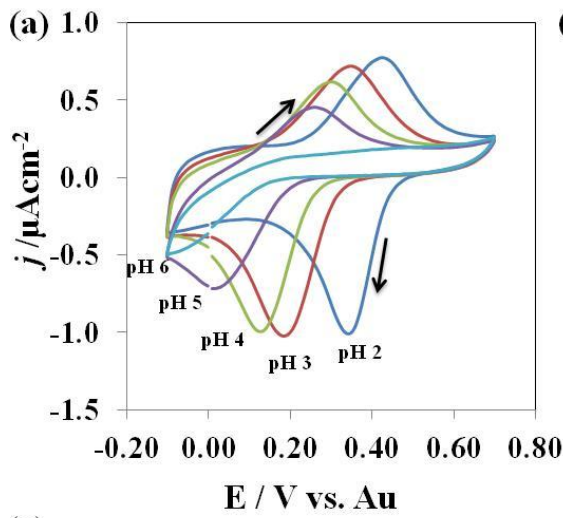


Fig. 1. CV at different pH (2~6) of (a) red, (b) rosé, and (c) white wines, recorded at a 0.0079 cm² PANI electrode at 0.05 vs. ⁻¹. The first scan of the CV was recorded each time. The pH was adjusted by adding NaOH /HCl to each wine. Calibration curve of (d) $E_{p,a}$ versus pH (red wine); (e) E^0 versus pH (rose wine) and (f) E^0 versus pH (white wine). Respective calibration curve made from CV.

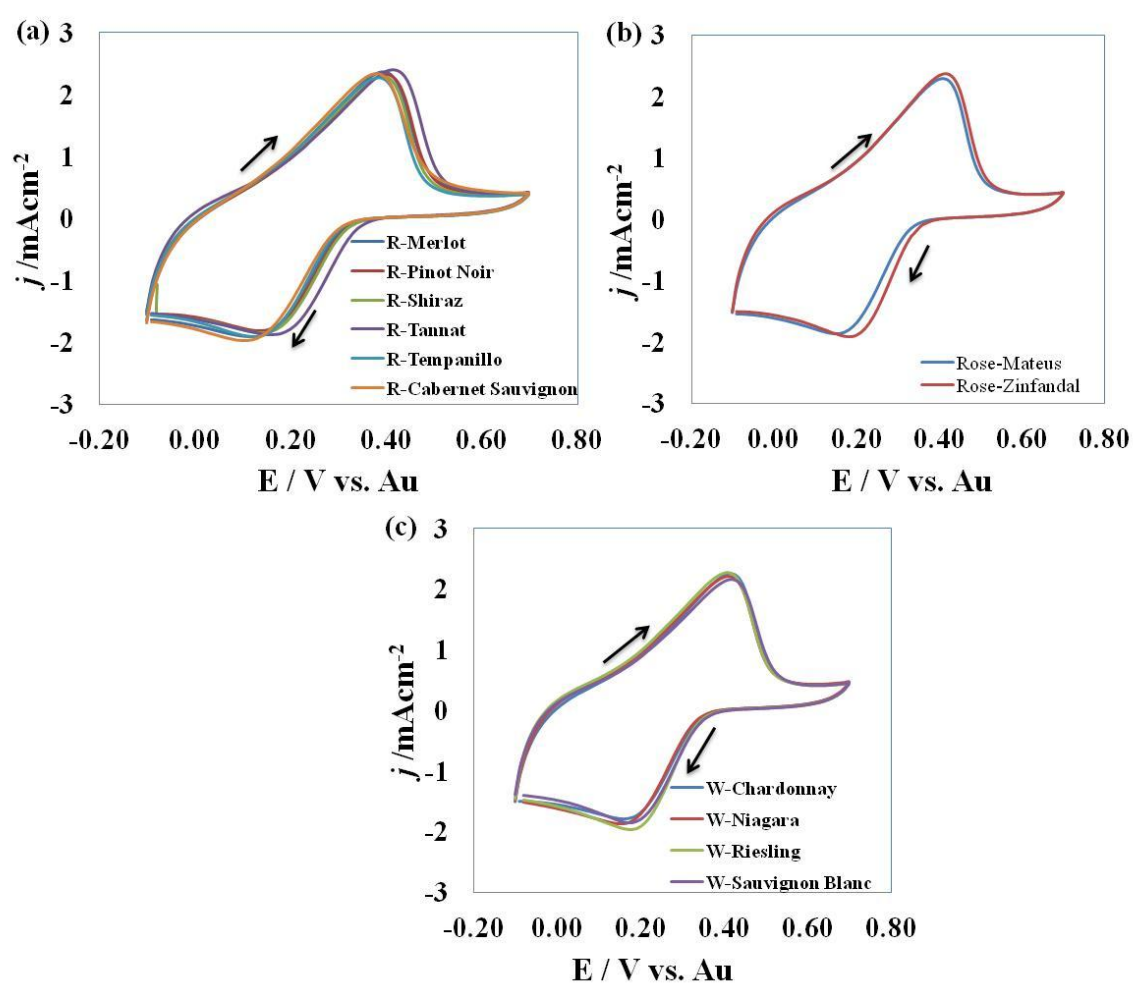


Fig. 2. Cyclic voltammograms of (a) red wines (Cabernet, Merlot, Pinor Noir, Shiraz, Tannot, Tempranillo, and Cabernet Sauvignon); (b) rose wines (Mateus and Zinfandal); (c) white wines (Chardonnay, Niagara, Riesling and Sauvignon Blanc) taken at a 0.0079

cm² PANI electrode at 0.05 Vs⁻¹ after opening. The first scan of the cyclic voltammogram was recorded for each sample.

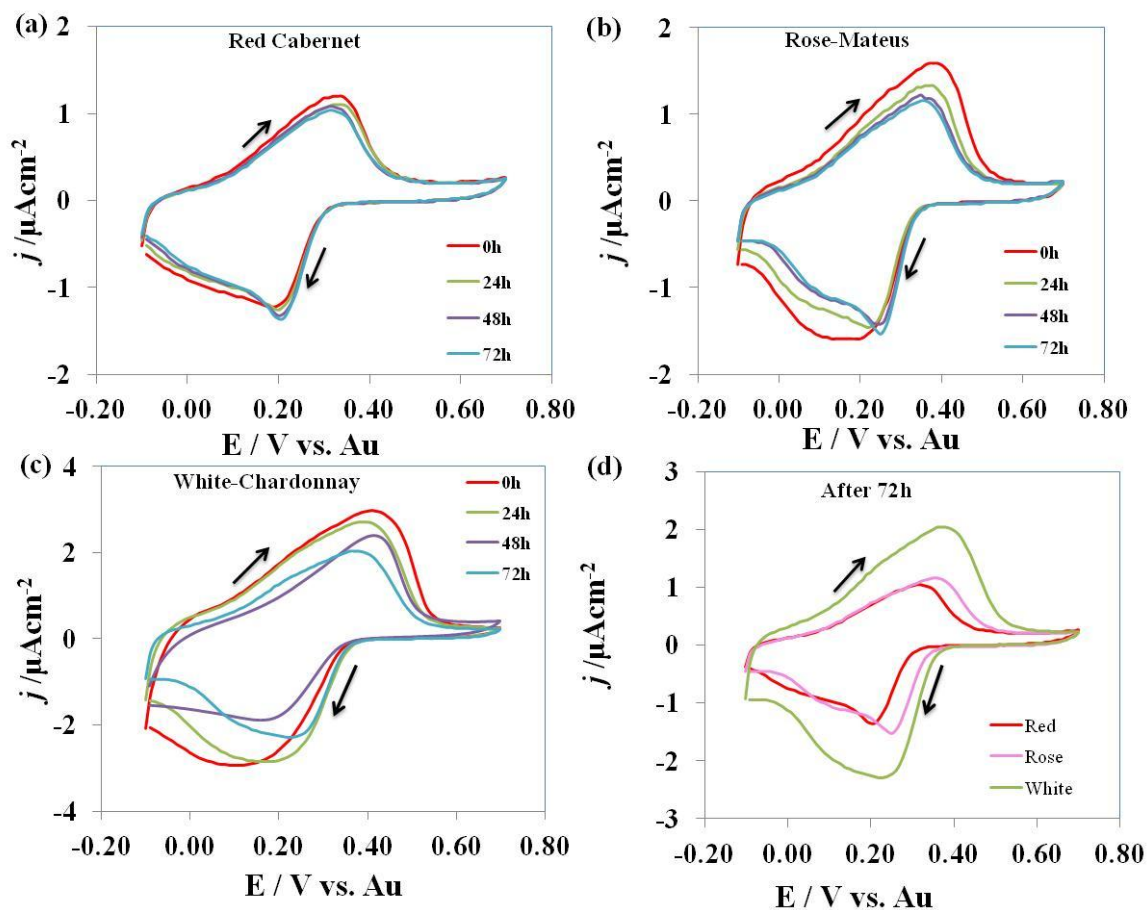


Fig. 3. CV of (a) red - Cabernate, (b) rose - Mateus, (C) white - Chardonnay, and (d) comparison of red, rose and white wines after opening at normal temperature (25 °C); recorded at a different time interval at a 0.0079 cm² PANI electrode at 0.05 Vs⁻¹. First scan of the cyclic voltammogram was recorded each time.

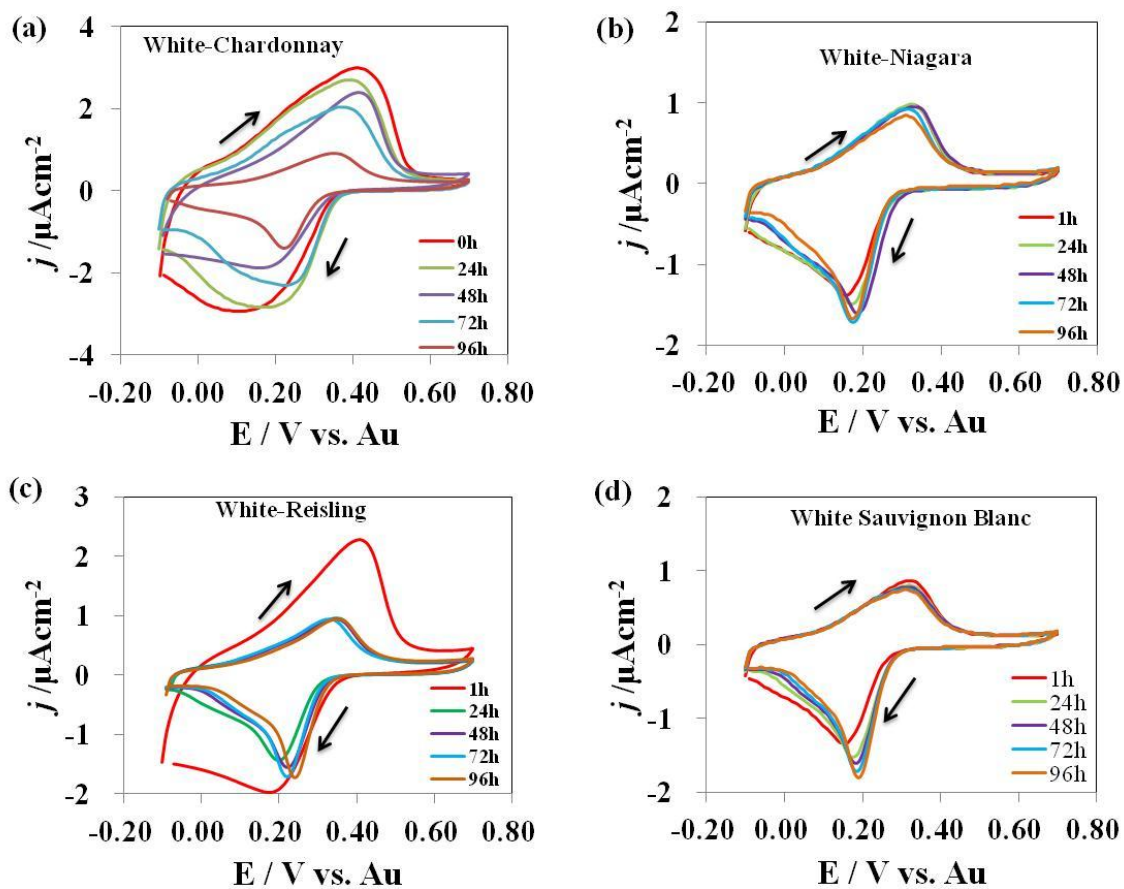


Fig. 4. CV of white wine (a) Chardonnay, (b) Niagara, (c) Reisling, and (d) Sauvignon Blanc after opening at normal temperature (25 °C); recorded at a different time interval at a 0.0079 cm² PANI electrode at 0.05 Vs⁻¹. First scan of the cyclic voltammogram was recorded each time.

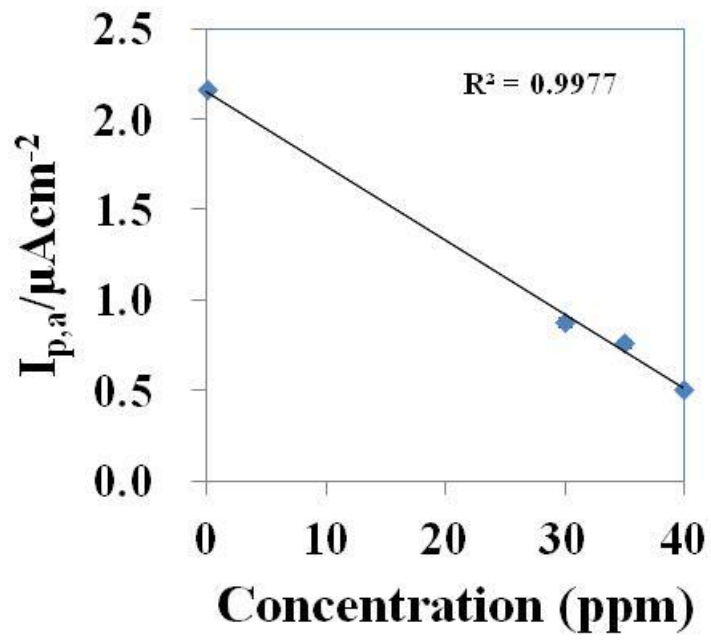


Fig. 5. Calibration curve of $I_{p,a}$ versus concentration of acetaldehyde (ppm).

Table 1. Information of wines accompanied with appearance/color and physiochemical parameters (pH, total acid, volatile acid and total sugar).

Wine	Grape variety	e	Appearance/ Color	pH	Total organic acids (g/l)	Volatile acids (g/l)	sugars (g/l)
Red	Santa Rita 3 Medallas Cabernet Sauvignon	2017	Ruby purple	3.61	3.2	0.41	2.7
	Merlot	2017	Ruby red	3.59	3.3	0.43	1.9
	Santa Helena Alpaca Pinot Noir	2017	Red purple	3.56	3.2	0.49	2.7
	Frontera Shiraz	2017	Ruby purple	3.58	3.3	0.48	5.6
	Tempranillo	2016	Ruby red	3.66	3.4	0.56	1.1
	Ascension Grand vin de Country Man Tannat	2016	Bright ruby purple	3.34	3.9	0.4	2.9
Rose	Mateus Rose	2016	Bright Rose	3.38	3.7	0.3	15.5
	Beringer White Zinfandal	2017	Rose	3.34	4.4	0.24	38.8
White	Santa Rita 3 Medallas Chardonnay	2017	Medium yellow	3.26	3.1	0.28	2
	Hokkaido Nama Wine Niagara	2017	Light yellow	3.33	4.1	0.38	3.2
	Riesling	2017	Light yellow	3.18	4.6	0.39	4.4
	Santa Helena Alpaca Sauvignon Blanc	2017	Light yellow	3.23	3.9	0.41	0.6

Highlights

- Sensing electrode was PANI modified Au electrode.
- Non-specific adsorption of organic compounds inhibited onto PANI electrode.
- Degradation of wine components observed by PANI sensor using CV.
- The $I_{p,a}$ and $E_{p,a}$ values shifted to a negative direction.

SUPPLEMENTARY MATERIAL FOR:

**PANI sensor for monitoring the oxidative degradation of wine using cyclic
voltammetry**

Parvin Begum^{a*}, Liu Yang^b, Tatsuya Morozumi^a, Teruo Sone^{b,c}, Toshikazu Kawaguchi^{a, b}

^a Faculty of Environmental Earth Sciences, Hokkaido University, Sapporo 060-0810, Japan

^b Graduate School of Global Food Resources, Hokkaido University, Sapporo 060-8589, Japan

^c Faculty of Agriculture, Hokkaido University, Sapporo 060-8589, Japan

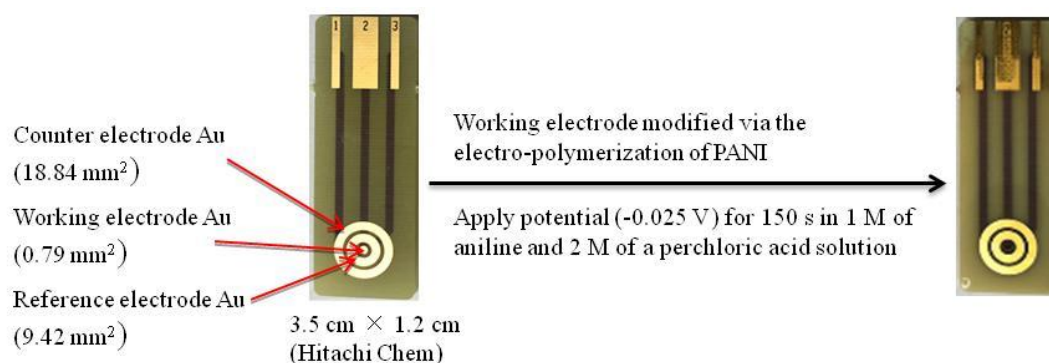
*Corresponding author

Email: parvinchy@ees.hokudai.ac.jp

Table of contents

Scheme SI-1 Preparation of electrochemical sensor chip	3
Gas Chromatography	3
Table S1-1 The electrochemical parameters extracted from CV of red, rose and white wines at different pH.....	4
Table SI-2 The electrochemical parameters extracted from CV of red, rose and white wines just after opening.....	4
Table SI-3 Comparison of the PANI electrode's determined detection limit in identifying the analytes of interest with recently published works.....	5
Fig. SI-1 CV of white wine (0 ppm, without acetaldehyde) and increasing amount of acetaldehyde (30 ppm, 35 ppm and 40 ppm); recorded at a 0.0079 cm ² PANI electrode at 0.05 Vs ⁻¹ . First scan of the cyclic voltammogram was recorded each time.....	5
Fig. SI-2 CV of two white wines (a) and (b) after opening at normal temperature (25 °C); recorded at different time interval at a 0.0079 cm ² PANI electrode at 0.05 Vs ⁻¹ . First scan of the cyclic voltammogram was recorded each time.....	6

Scheme SI-1 Preparation of electrochemical sensor chip



Gas Chromatography:

The wine was analyzed on a gas chromatograph with a flame ionization detector (GC-FID) using a SHIMADZU GC-2025 chromatograph equipped with a Zebron (ZB-5 5% phenyl, 95% dimethylpolysiloxane) capillary column (30 m × 0.25 mm × 0.25 μm); an AOC-20i autosampler; and a split–splitless injector (SHIMADZU 09427). To assign the peaks of metabolized products according to mass fragmentation profiles, the system was equipped with a gas chromatograph–mass spectrometer (SHIMADZU GCMS-QP2010SE). The temperatures of the injector and detector were set at 200 and 250 °C, respectively. The oven temperature was first maintained at 40 °C for 10 min, after which it was increased at a rate of 10 °C/min to 250 °C and finally held at this temperature for 5 min. Thereafter, 1 μL of each sample was injected in the splitless mode (25 s). Helium was the carrier gas at a constant flow rate of 48.5 mL/min.

Table SI-1 The electrochemical parameters extracted from CV of red, rose and white wines at different pH

Red	pH	$E_{p,a} / V$	$I_{p,a} / \mu Acm^{-2}$	$E_{p,c} / V$	$(-) I_{p,c} / \mu Acm^{-2}$	$\Delta E_p / V$	$\Delta I_p / \mu Acm^{-2}$	$I_{p,a} / I_{p,c}$	$E_0 = (E_{p,a} + E_{p,c}) / 2$
	2	$0.429 \pm 0.04c$	$7.711 \pm 0.02a$	$0.339 \pm 0.02d$	$128.012 \pm 0.02a$	0.091	30.301	0.763	0.384
	3	$0.349 \pm 0.02a$	$1.269 \pm 0.02a$	$0.199 \pm 0.03b$	$26.525 \pm 0.03b$	0.150	35.257	0.721	0.274
	4	$0.310 \pm 0.04c$	$8.137 \pm 0.02a$	$0.129 \pm 0.03b$	$25.782 \pm 0.03b$	0.180	47.646	0.621	0.219
	5	$0.259 \pm 0.03b$	$7.819 \pm 0.04c$	$0.019 \pm 0.02a$	$90.846 \pm 0.03b$	0.240	33.027	0.636	0.139
Rose	2	$0.250 \pm 0.02a$	$4.509 \pm 0.04c$	$0.160 \pm 0.02a$	$177.071 \pm 0.04c$	0.090	112.562	0.364	0.205
	3	$0.250 \pm 0.02a$	$1.694 \pm 0.02a$	$0.120 \pm 0.04d$	$58.736 \pm 0.04c$	0.130	87.042	0.452	0.185
	4	$0.240 \pm 0.02a$	$6.650 \pm 0.02a$	$0.060 \pm 0.02a$	$31.976 \pm 0.03b$	0.180	55.327	0.581	0.150
	5	$0.220 \pm 0.04c$	$6.402 \pm 0.02a$	$0.021 \pm 0.02a$	$98.279 \pm 0.04c$	0.199	21.877	0.777	0.120
White	2	$0.360 \pm 0.03b$	$8.384 \pm 0.02a$	$0.260 \pm 0.03b$	$162.700 \pm 0.02a$	0.100	84.315	0.482	0.310
	3	$0.330 \pm 0.04c$	$3.924 \pm 0.04c$	$0.180 \pm 0.02a$	$159.479 \pm 0.03b$	0.150	85.555	0.464	0.255
	4	$0.280 \pm 0.02a$	$4.509 \pm 0.02a$	$0.109 \pm 0.03b$	$33.711 \pm 0.04c$	0.170	69.202	0.482	0.194
	5	$0.260 \pm 0.03b$	$2.120 \pm 0.02a$	$0.019 \pm 0.03b$	$92.085 \pm 0.04c$	0.240	39.965	0.566	0.139

Note: Values (means \pm SD) bearing different superscripts are statistically significantly different ($P \leq 0.01$)

Table SI-2 The electrochemical parameters extracted from CV of red, rose and white wines just after opening.

	Wine Name	$E_{p,a} / V$	$I_{p,a} / \mu Acm^{-2}$	$E_{p,c} / V$	$(-) I_{p,c} / \mu Acm^{-2}$	$\Delta E_p / V$	$\Delta I_p / \mu Acm^{-2}$	$I_{p,a} / I_{p,c}$	$E_0 = (E_{p,a} + E_{p,c}) / 2$
Red	Tannat	$0.409 \pm 0.01a$	$303.797 \pm 0.03a$	$0.159 \pm 0.03c$	$238.024 \pm 0.01a$	0.250	65.772	1.276	0.284
	Merlot	$0.389 \pm 0.01a$	$299.114 \pm 0.03a$	$0.119 \pm 0.03c$	$240.750 \pm 0.01a$	0.270	58.364	1.242	0.254
	Cabernet Sauvignon	$0.379 \pm 0.03c$	$295.57 \pm 0.02b$	$0.109 \pm 0.02b$	$249.173 \pm 0.03a$	0.270	46.397	1.186	0.244
	Pinot Noir	$0.399 \pm 0.02a$	$293.418 \pm 0.01a$	$0.129 \pm 0.01a$	$229.104 \pm 0.03a$	0.270	64.314	1.280	0.264
	Shiraz	$0.389 \pm 0.02a$	$290.127 \pm 0.01a$	$0.139 \pm 0.01a$	$234.060 \pm 0.01a$	0.250	56.067	1.240	0.264
Rose	Tempanillo	$0.379 \pm 0.02a$	$286.203 \pm 0.02b$	$0.130 \pm 0.02b$	$240.502 \pm 0.02b$	0.250	45.701	1.190	0.254
	Zinfandal	$0.409 \pm 0.02b$	$299.367 \pm 0.03a$	$0.179 \pm 0.03c$	$242.980 \pm 0.02b$	0.230	56.387	1.232	0.294
White	Mateus	$0.409 \pm 0.02b$	$290.38 \pm 0.02b$	$0.149 \pm 0.01a$	$236.289 \pm 0.01a$	0.260	54.091	1.229	0.279
	Riesling	$0.409 \pm 0.03c$	$288.481 \pm 0.01a$	$0.169 \pm 0.02b$	$248.431 \pm 0.01a$	0.240	40.050	1.161	0.289
	Chardonnay	$0.419 \pm 0.01a$	$284.43 \pm 0.01a$	$0.139 \pm 0.02b$	$225.387 \pm 0.03a$	0.280	59.043	1.262	0.279
	Niagara	$0.419 \pm 0.03c$	$277.342 \pm 0.03a$	$0.149 \pm 0.01a$	$237.033 \pm 0.03a$	0.270	40.309	1.170	0.284
	Sauvignon Blanc	$0.419 \pm 0.02b$	$273.291 \pm 0.01a$	$0.179 \pm 0.03c$	$233.564 \pm 0.02b$	0.240	39.727	1.170	0.299

Note: Values (means \pm SD) bearing different superscripts are statistically significantly different ($P \leq 0.01$)

Table SI-3 Comparison of the PANI electrode's determined detection limit in identifying the analytes of interest with recently published works.

Sensor	Detection limi	Analytes	Ref.
GCE/PANI/GNPs	0.1 mM	Glucose	Ahammad et al. 2016
Hb/PANI-TiC/GCE	0.2 μ M	H ₂ O ₂	Zhang et al. 2014
PANI	0.8816 mM	Cadaverine	Ocampo et al. 2018
PANI	500 ppm	Toxic gas	Hosseini et al. 2005
PANI/Ag	1.24 ppm	Formaldehyde vapor	Zhang et al. 2016
PANI(IO)	29 ppm	Acetone gas	Do et al. 2013
PANI	7×10^{-1} ppm	Acetaldehyde	This work

Note: polyaniline-modified glassy carbon electrode- gold nanoparticles (GCE/PANI/GNPs) for the detection of glucose; Hemoglobin- polyaniline-titanium carbide-glassy carbon electrode (Hb/PANI-TiC/GCE) for the reduction of H₂O₂; PANI for the detection of cadaverine; polyaniline (PANI) for the detection of toxic gas; polyaniline/silver nanocomposite (PANI/Ag) for the determination of formaldehyde vapor; polyaniline/impregnated oxidation technique (PANI(IO)) for the detection of acetone gas.

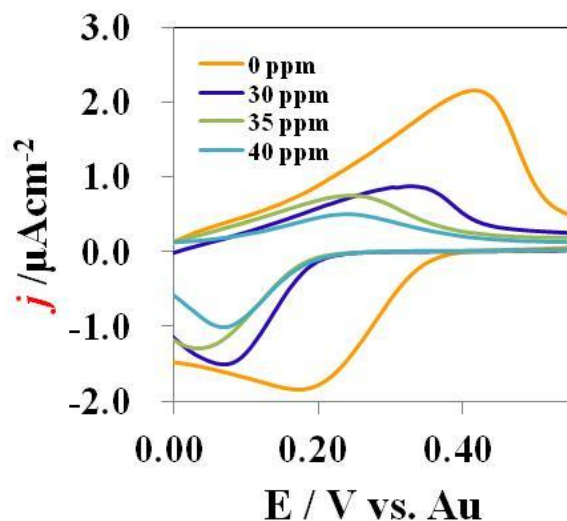


Fig. SI-1 CV of white wines (0 ppm, without acetaldehyde) and increasing amount of acetaldehyde (30 ppm, 35 ppm and 40 ppm); recorded at a 0.0079 cm² PANI electrode at 0.05 Vs⁻¹. First scan of the cyclic voltammogram was recorded each time.

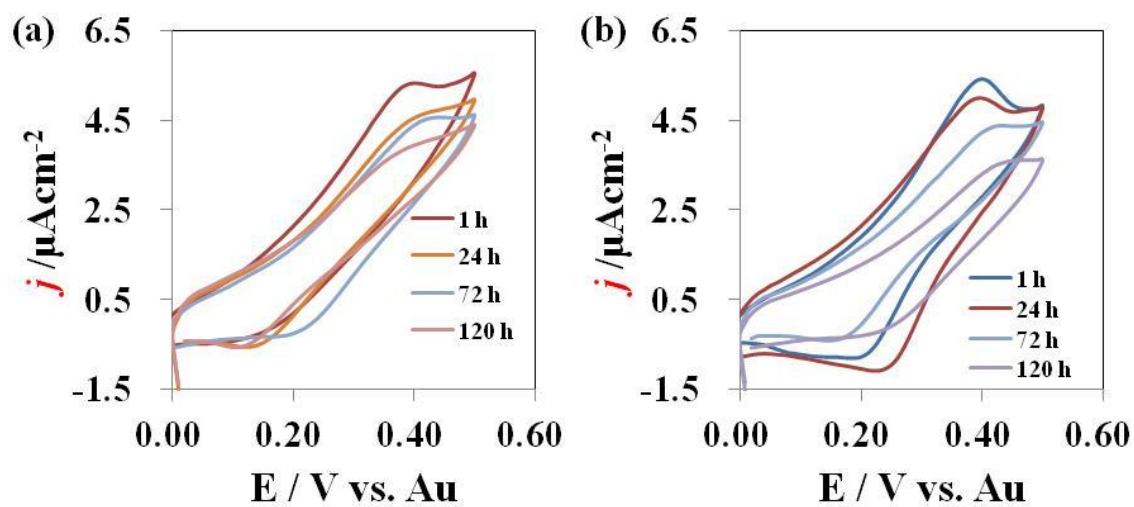


Fig. SI-2 CV of two white wines (a and b) after opening at normal temperature (25 °C); recorded at different time interval at a 0.0079 cm^2 PANI electrode at 0.05 Vs^{-1} . First scan of the cyclic voltammogram was recorded each time.